DOI: 10.6060/ivkkt.20256810.7231

ВЛИЯНИЕ МОЩНОСТИ МИКРОВОЛНОВОГО ОБЛУЧЕНИЯ НА ПРОИЗВОДСТВО ФТОРАПАТИТА ИЗ ОТХОДОВ ЯИЧНОЙ СКОРЛУПЫ МЕТОДОМ ХИМИЧЕСКОГО СООСАЖДЕНИЯ

Г.Р. Колчакова, Д.С. Кирякова

Ганка Румянова Колчакова (ORCID 0000-0001-9174-6550)*, Димитрина Стоянова Кирякова (ORCID 0000-0002-2742-2399)

Кафедра материаловедения, Университет Асена Златарова, Бульв. Якима Якимова, 1, Бургас, Болгария, 8010
E-mail: gkolchakova@gmail.com*, dskiryakova@abv.bg

В этом исследовании изучалось влияние мощности микроволнового облучения на синтез фторапатита (FAp) из отходов яичной скорлупы с использованием метода химического соосаждения. Смесь прекурсоров подвергалась микроволновой обработке при уровнях мощности 600 и 800 Вт. Для оценки характеристик синтезированных порошков использовались методы рентгеновской дифракции (XRD), инфракрасной Фурье-спектроскопии (FTIR) и сканирующей электронной микроскопии (SEM). Результаты показали, что при 600 Вт получается двухфазный материал, содержащий основную фазу монетит и вторичную фазу фторапатит, в то время как при 800 Вт наблюдается получение чистого фторапатита.

Ключевые слова: мощность микроволнового излучения, отходы яичной скорлупы, фторапатит, монетит, химическое соосаждение

INFLUENCE OF MICROWAVE IRRADIATION POWER ON THE PRODUCTION OF FLUORAPATITE FROM WASTE EGGSHELLS BY CHEMICAL CO-PRECIPITATION

G.R. Kolchakova, D.S. Kiryakova

Ganka R. Kolchakova (ORCID 0000-0001-9174-6550)*, Dimitrina S. Kiryakova (ORCID 0000-0002-2742-2399)

Department of Material Science, Assen Zlatarov University, Yakim Yakimov st., 1, Burgas, Bulgaria, 8010
E-mail: gkolchakova@gmail.com*, dskiryakova@abv.bg

This study investigated the effect of microwave irradiation power on the synthesis of fluorapatite (FAp) from waste eggshells using a chemical coprecipitation method. The precursor mixture was subjected to microwave treatment at power levels of 600 and 800 W. X-ray diffraction (XRD), Fourier transform infrared (FTIR), and Scanning electron microscopy (SEM) analysis techniques were utilized to evaluate the characteristics of synthesized powders. The results showed that at 600 W a two-phase material is obtained, containing a main phase monetite and a secondary phase fluorapatite, while at 800 W the production of pure fluorapatite is observed.

Keywords: microwave irradiation power, waste eggshells, fluorapatite, monetite, chemical co-precipitation

Для цитирования:
Колчакова Г.Р., Кирякова Д.С. Влияние мощности микроволнового облучения на производство фторапатита из отходов яичной скорлупы методом химического соосаждения. *Изв. вузов. Химия и хим. технология*. 2025. Т. 68. Вып. 10. С. 81–86. DOI: 10.6060/ivkkt.20256810.7231.

For citation:
Kolchakova G.R., Kiryakova D.S. Influence of microwave Irradiation power on the production of fluorapatite from waste eggshells by chemical co-precipitation. *ChemChemTech [Izv. Vyssh. Uchebn. Zaved. Khim. Khim. Tekhnol.]*. 2025. V. 68. N 10. P. 81–86. DOI: 10.6060/ivkkt.20256810.7231.

INTRODUCTION

Fluorapatite (FAp) is a calcium phosphate mineral characterized by high biocompatibility, chemical resistance, and excellent mechanical strength [1-2]. The stability and insolubility of fluorapatite in physiological fluids are due to the presence of fluoride ions, which significantly improve chemical and thermal resistance [3]. These characteristics make it extremely attractive for applications in dental and orthopedic regeneration [4-5], catalysis [6-7], water treatment [8-9], and phosphate fertilizer production [8, 10].

A sustainable approach to the synthesis of fluorapatite involves the use of natural, calcium-containing, biogenic wastes as raw material sources. For instance, Erlanga et al. [11] successfully synthesized fluorapatite from the shells of the golden snail (Pomacea canaliculata) by precipitation and solid-state reaction methods. Similarly, Graziani et al. [4] used seashells from Lingula anatine – materials characterized by a high content of calcium carbonate ($CaCO_3$) – to develop biomaterials for orthopedic and dental applications. In this context, the use of waste eggshells is a promising approach that will not only reduce waste and the environmental footprint, but also offers an economical alternative to traditional raw materials [12-14]. Although there is insufficient literature on the synthesis of fluorapatite from eggshells, they show promising results in terms of its structural properties, biocompatibility and potential applications in bone regeneration and dentistry [11, 15].

In the quest to achieve optimal properties of biomaterials, scientists have developed a wide range of synthesis methods that allow for more precise control over the morphology, purity, and crystal structure of the final product. These include precipitation methods [1], hydrothermal processes [16-17], sol-gel methods [3], and mechanochemical approaches [18-19], each of which has an impact on the characteristics of the final product and poses a significant challenge in optimizing the reaction conditions. Recently, researchers have increasingly turned to the use of microwave heat as an alternative source of thermal energy, which offers a number of advantages - rapid and uniform heating, improved reaction kinetics, shortened synthesis time, and increased yields [20-23]. This integrated approach, combining sustainable raw materials with innovative synthesis techniques [24], promises significant improvements in the development of high-quality biomaterials.

The aim of this research is to synthesize fluorapatite from waste eggshells as a low-cost source of calcium using the chemical co-precipitation method followed by microwave heating. Unlike previous studies that employed lower microwave powers and required additional thermal treatments to achieve phase purity and crystallinity, this study investigates the effect of higher microwave irradiation powers (600 and 800 W) on the direct formation of single-phase, highly crystalline fluorapatite. By eliminating the need for further heat treatment, this approach enhances energy efficiency and sustainability.

EXPERIMENTAL

For synthesis of fluorapatite powders utilizes waste eggshells, phosphoric acid (H_3PO_4, 85%), and sodium fluoride (NaF, 99%), products of Sigma-Aldrich. Initially, the eggshells are washed, air-dried for 24 h, and then dried at 105 °C until a constant weight is achieved. They are processed using a planetary ball mill ("Pulverisette 6") and fractionated with a vibratory sieve shaker ("Retsch AS 200"). Laboratory test sieves with nominal apertures from 100 μm to 25 μm (ISO 3310-1) were used for the sieve analysis. For the experiment, the predominant fraction, $71 \geq 50$ μm, was selected. The eggshell powder was subjected to thermal treatment at 900 °C for 2 h. During the calcination process, the main inorganic component ($CaCO_3$) underwent thermal decomposition. Carbon dioxide is released, and calcium oxide (CaO) is formed [23]. The resulting CaO was dissolved in the required amount of distilled water to form $Ca(OH)_2$.

In order to prepare the precursor calcium phosphate ($Ca_3(PO_4)_2$), we added a 1M phosphoric acid solution to the calcium base (eq. 1), ensuring a pH of 7 to optimize precipitation [25]. For the formation of fluorapatite, a stoichiometric amount of 2% sodium fluoride solution was added to ensure uniformity and prevent the formation of a side phase. The reaction was carried out for 2 h at 90°C with continuous stirring (eq. 2).

$$3Ca(OH)_2+2H_3PO_4 \rightarrow Ca_3(PO_4)_2+6H_2O \quad (1)$$

$$3Ca_3(PO_4)_2+Ca(OH)_2+2NaF \rightarrow$$
$$\rightarrow 2Ca_5(PO_4)_3F+2NaOH. \quad (2)$$

After the reaction, the mixture is left at room temperature for 24 h for precipitation. The precipitate is filtered, washed to remove sodium and ammonium ions, and dried at 105 °C for 12 h. The powders underwent microwave irradiation power at 600W and 800W for 45 min to complete the synthesis using a commercial household microwave „Sharp“(900 W, 2450 MHz; China).

Characterization

X-ray diffraction (XRD) was employed to identify the crystal structure of obtained powders,

while Fourier-transform infrared spectroscopy (FTIR) was utilized to analyze the chemical composition. Scanning electron microscopy (SEM) was used to determine the morphology, particle size, and surface structure of the obtained samples.

XRD (X-Ray Diffraction) characterization was carried out on a powder diffractometer Bruker 2D Phaser. The samples were irradiated with CuKα irradiation (λ = 1.54060 Å) and analyzed between 2-90° (2 theta).

Fourier transform infrared spectroscopy (FTIR) is a tool for identifying the types of chemical bonds in organic and inorganic molecules. Analysis is performed by using the spectrophotometer Nicolet iS 50 FT-IR Thermo Scientific in the interval 4000-400 cm^{-1}.

Scanning electron microscopy was performed on a JSM 6390 electron microscope (Japan) in conjunction with energy dispersive X-ray spectroscopy (EDS, Oxford IN-CA Energy 350) equipped with an ultrahigh resolution scanning system (ASID-3D) in regimes of secondary electron image and back scattered electron image.

RESULTS AND DISCUSSION

To investigate the phase purity and composition of the synthesized powders subjected to various microwave treatments, X-ray powder diffraction (XRD) analysis was performed (Figs. 1 and 2). The XRD profile of the sample produced through chemical co-precipitation and subsequently heated in a microwave power at 600W (Fig. 1) reveals the presence of two phases within the synthesized powder. Notable diffraction peaks at 2θ angles of 26.42°, 26.58°, and 30.18° are characteristic of monetite (CaHPO4) [26], corresponding to the crystal lattice planes: 020, -220, and -112.

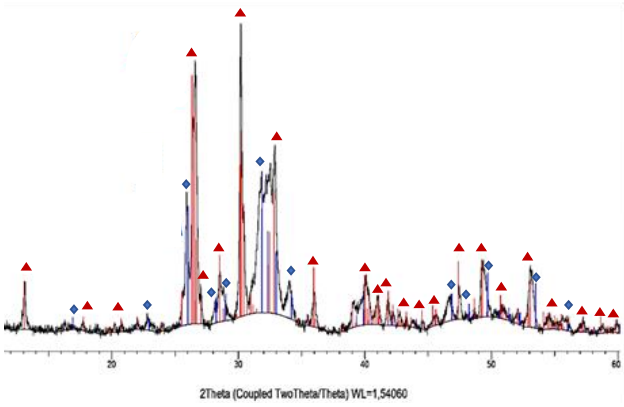

Fig. 1. XRD diffractogram of calcium-containing powders obtained by microwave irradiation at 600W: $CaHPO_4$ (♦); $Ca_5(PO_4)_3F$ (▲)

Рис. 1. Дифрактограмма кальцийсодержащих порошков, полученных при микроволновом облучении мощностью 600 Вт: $CaHPO_4$ (♦); $Ca_5(PO_4)_3F$ (▲)

In contrast, the diffraction peaks observed at 2θ values of 25.99°, 32.25°, 33.04°, 46.84°, 49.57°, and 53.23° indicate the presence of a crystalline fluorapatite phase ($Ca_5(PO_4)_3F$ [27]. The XRD pattern of the sample subjected to microwave heating at a power of 800 W (Fig. 2), demonstrating that the resulting powder is a single-phase crystalline fluorapatite. The characteristic peaks for fluorapatite are more pronounced, with additional peaks appearing at 2θ values of 28.16°, 29.05°, 34.13°, 39.29°, 39.97°, 42.15°, 44.56°, and 48.79°. The corresponding Miller indices (hkl) for these peaks are (102), (120), (202), (122), (310), (311), (400), and (320). These findings are consistent with the standard reference card for fluorapatite (JCPDS 15-0876), confirming the purity of the fluorapatite phase in the synthesized powder [20].

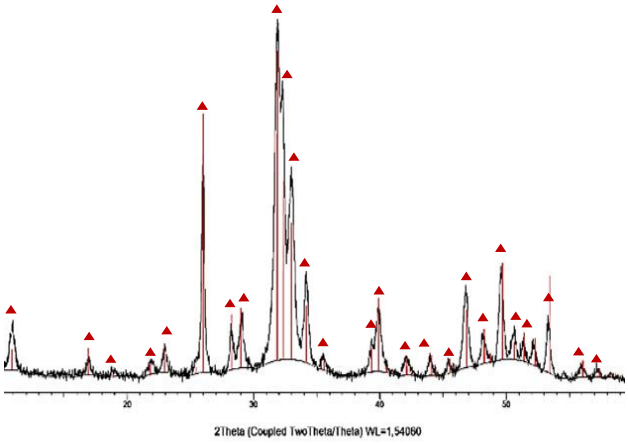

Fig. 2. XRD diffractogram of fluorapatite obtained by microwave irradiation at 800W

Рис. 2. Дифрактограмма фторапатита, полученных при микроволновом облучении мощностью 800 Вт

The results of the XRD analysis confirmed that microwave treatment is essential for achieving a pure phase in the synthesized material. Although fluorapatite is primarily formed during co-precipitation, it may contain small intermediate phases or unreacted precursors. Using a microwave power of 600 W does not provide enough heat for the full conversion of the reactants into fluorapatite (Fig. 1), leading to the formation of a two-phase system mainly consisting of monetite (63.8%) and fluorapatite (36.2%). When heated at 800 W, the reaction temperature increases, which enhances the mobility of calcium, phosphate, and fluoride ions [3] and reduces the barriers to diffusion. The higher microwave power, and consequently the higher temperature stimulates the formation of the most stable phase - pure fluorapatite. Additionally, the increased intensity in the XRD pattern at higher powers (Fig. 2) shows that the material's crystallinity has improved

[26], confirming the effectiveness of microwave heating. These results are consistent with previous studies, which indicate that microwave synthesis can effectively produce well-crystallized fluorapatite without the need for additional heating or sintering processes [23].

The influence of microwave irradiation power on the synthesis of fluorapatite was confirmed by FT-IR analysis. Fig. 3 presents a comparative overview of the FT-IR spectra, while Table 1 summarizes the identified vibrational modes.

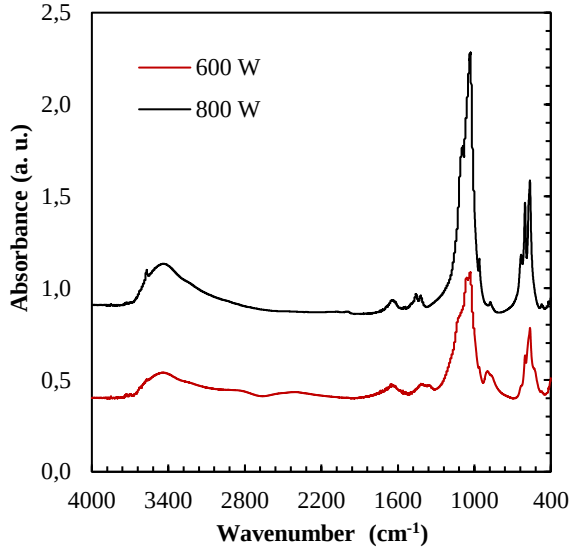

Fig. 3. FT–IR spectra of synthesized calcium-containing powders at different microwave irirradiation

Рис. 3. ИК-спектры синтезированных кальцийсодержащих порошков при различной мощности микроволнового облучения

The spectral analysis of the sample heated at microwave power at 800 W (Fig. 3) confirms the formation of crystalline fluorapatite with a well-defined phase composition. The dominant band at 1030 cm^{-1}, with a shoulder at 1090 cm^{-1}, corresponds to the asymmetric stretching mode of the PO_4^{3-} group, while the peaks at 562 and 601 cm^{-1} are associated with the asymmetric bending vibrations of the phosphate tetrahedra [27]. The appearance of a doublet at 1430 and 1450 cm^{-1}, reveals the presence of carbonated groups, signifying B-type substitution in which CO_3^{2-} ions replace PO_4^{3-} groups [4]. This structural modification enhances the bioactivity and biocompatibility of the material, making it particularly suitable for biomedical applications such as bone tissue engineering [28]. Additionally, the presence of a band at 960 cm^{-1}, attributed to PO_4 vibrations to the deprotonation of HPO_4 groups, further confirm the formation of the apatite structure [18].

The FT-IR spectrum of the sample heated at 600 W displays a more complex vibrational profile, confirming the results obtained from XRD analysis. The characteristic band at 1030 cm^{-1}, corresponding to the stretching of the PO_4^{3-} group, is less pronounced, suggesting weak crystallinity and an incomplete transformation of the precursor phases. The presence of monetite is further indicated by a weak band at 529 cm^{-1}, which corresponds to the HO–PO_3 bending vibration of HPO_4^{2-} groups [29]. Additionally, peaks observed at 881 and 1380 cm^{-1} are attributed to P–OH stretching vibrations and P–OH in-plane bending, in within these groups, respectively [30]. Finally, bands at 2870 and 2350 cm^{-1}, associated with O–H stretching vibrations of HPO_4^{2-} , further confirm the incorporation of monetite into the phase composition of the sample [31].

Table

The characteristic frequencies (cm^{-1}) and assignments for synthesized powders from infrared spectrum

***Таблица*. Характерные частоты ($см^{-1}$) и отнесения для синтезированных порошков из инфракрас-ного спектра**

Infrared peaks (cm^{-1})	Assignments	Microwave irradiation	
		600 W	800 W
529	v_4 PO bending	×	
562, 601	v_4 PO bending	×	×
881	P-O(H) stretching	×	
960	v_1 PO stretching		×
1030, 1090	v_3 PO stretching	×	×
1380	P-OH in-plane bending	×	
1430, 1450	v_3 CO_3 stretching	×	×
2350, 2870	OH stretching	×	

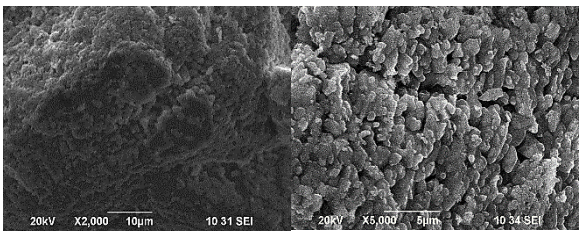

Fig. 4. SEM images of fluorapatite ($Ca_5(PO_4)_3F$)

Рис. 4. СЭМ фотографии фторапатит ($Ca_5(PO_4)_3F$)

A scanning electron microscopy (SEM) analysis was performed to investigate the morphology and dimensions of fluorapatite particles synthesized via 800 W microwave irradiation. The SEM images, as depicted in Fig. 4, reveal a uniform microstructure characterized by rod-shaped particles exhibiting smooth surfaces, free from porosities or defects, indicative of complete crystallization. The average particle size ranges from 1 to 3 μm, with a pronounced tendency for agglomeration. In comparison to the conventional method, which involves high-temperature sintering

over extended periods as described by Khofiyatuzziyadah et. all and Erlanga et. all [1, 11], the microwave approach offers significantly faster processing and enhanced energy efficiency while maintaining effective control over the crystallization process. Although both methods present a similar morphology and agglomeration levels, the microwave synthesis minimizes prolonged exposure to high temperatures.

CONCLUSION

This study demonstrates that microwave irradiation power is a critical parameter in the synthesis of fluorapatite ($Ca_5(PO_4)_3F$) powders, significantly influencing reaction completeness, phase composition, and crystallinity. At 600 W, the reaction remains incomplete, yielding a heterogeneous material dominated by monetite ($CaHPO_4$), indicative of insufficient energy to fully transform precursor phases. In contrast, the application of higher microwave power (800 W) enhances reaction kinetics and ion diffusion, resulting in the complete formation of pure fluorapatite with a particle size of 1-3 μm. The aggregation of particles emphasizes the need to optimize microwave irradiation parameters to control material properties.

Microwave-assisted synthesis of fluorapatite from waste eggshells demonstrates significant application potential, combining economic efficiency and environmental sustainability. The main advantage of the method is a significant reduction in synthesis time and energy consumption, inherent in high-temperature processing in conventional methods. The applied value of the method is complemented by the use of biowaste eggshells as an alternative source of calcium. This approach not only reduces raw material costs but also implements the principles of the circular economy by transforming waste material into a valuable resource and contributing to sustainable waste management.

ACKNOWLEDGEMENTS

This work was supported by the Scientific Research Center at Assen Zlatarov University under the contract № 495/2024.

The authors declare the absence of a conflict of interest warranting disclosure in this article.

Работа выполнена при поддержке Научно-исследовательского центра Университета Асена Златарова в рамках контракта № 495/2024.

Авторы заявляют об отсутствии конфликта интересов, требующего раскрытия в данной статье.

REFERENCES
ЛИТЕРАТУРА

1. **Khofiyatuzziyadah A., Charlena C., Maddu A.** // *Mat. Int.* 2024. V. 6. P. 32. DOI: 10.33263/Materials64.032.
2. **Seyedmajidi S., Seyedmajidi M.** // *Iran. J. Mater. Sci. Eng.* 2022. V. 19. P. 1-20. DOI: 10.22068/ijmse.2430.
3. **Charlena C., Sari Y., Islamia W.** // *Indones. J. Pure Appl. Chem.* 2023. V. 6. P. 152. DOI: 10.26418/indonesian.v6i3.67697.
4. **Graziani G., Ghezzi D., Nudelman F., Sassoni E., Laidlaw F., Cappelletti M., Borchiani G., Milita S., Bianchi M., Baldini N., Falini G.** // *J. Mater. Chem. B.* 2024. V. 12. P. 2083–2098. DOI: 10.1039/d3tb02454g.
5. **Jeong J., Kim J.H., Shim J.H., Hwang N.S., Heo C.Y.** // *Biomat. Res.* 2019. V. 23. P. 4. DOI: 10.1186/s40824-018-0149-3.
6. **Essamlali Y., Amadine O., Fihri A., Zahouily M.** // *Renew. Energy.* 2019. V. 133. P. 1295–1307. DOI: 10.1016/j.renene.2018.08.103.
7. **Vishwakarma R., Mannepalli L.K., Rathod V.** // *Chem. Eng. Res. Des.* 2022. V. 181. 101–109. DOI: 10.1016/j.cherd.2022.03.001.
8. **Xia Y., Huang X., Li W., Zhang Y., Li Z.** // *J. Hazard. Mater.* 2019. V. 361. P. 321–328. DOI: 10.1016/j.jhazmat.2018.09.007.
9. **Ma L., Huang Y., Zhao K., Deng H., Tian Q., Yan M.** // *J. Environ. Chem. Eng.* 2021. V. 9. P. 106600. DOI: 10.1016/j.jece.2021.106600.
10. **Ramteke L., Sahayam A., Ghosh A., Rambabu U., Reddy M., Popat K., Rebary B., Kubavat D., Marathe K., Ghosh P.** // *J. Fluor. Chem.* 2018. V. 210. P. 149–155. DOI: 10.1016/j.jfluchem.2018.03.018.
11. **Erlangga M., Charlena C., Suparto I.** // *J. Kim. Sains Apl.* 2024. V. 27. P. 174-181. DOI: 10.14710/jksa.27.4.174-181.
12. **Baláž M., Boldyreva E.V., Rybin D., Pavlović S., Rodríguez-Padrón D., Mudrinić T., Luque R.** // *Front. Bioeng. Biotechnol.* 2021. V. 8. P. 612567. DOI: 10.3389/fbioe.2020.612567.
13. **Pagonis N., Flegkas D., Itziou A., Kountouras K., Stimoniaris A., Samaras P., Karayannis V.** // *Eng.* 2024. V. 5. P. 3540–3550. DOI: 10.3390/eng5040184.
14. **Torres G.M.E., Milhans C., Gezek M., Camci-Unal G.** // *Adv. NanoBiomed Res.* 2024. P. 2400120. DOI: 10.1002/anbr.202400120.
15. **Nuzulia N., Bachtiar, E., Alisyah D., Sari Y.** // *AIP Conf. Proc.* 2024. 3210. P. 020005. DOI: 10.1063/5.0227909.
16. **Nuzulia N., Siregar F., Sari Y.** // *AIP Conf. Proc.* 2021. 2346. P. 020008. DOI: 10.1063/5.0048192.
17. **Taheri M., Shirdar M., Keyvanfar A., Shafaghat A.** // *J. Exp. Nanosci.* 2016. V. 12. P. 83–93. DOI: 10.1080/17458080.2016.1263400.
18. **Bulina N., Makarova S., Prosanov I., Vinokurova O., Lyakhov N.** // *J. Solid State Chem.* 2020. V. 282. P. 121076. DOI: 10.1016/j.jssc.2019.121076.
19. **Fereshteh Z., Fathi M., Mozaffarinia R.** // *J. Clust. Sci.* 2015. V. 26. P. 1041–1053. DOI: 10.1007/s10876-014-0793-2.
20. **Tiskute M., Eisinas A., Baltakys K.** // *J. Therm. Anal. Calorim.* 2025. V. 150. P. 977-989. DOI: 10.1007/s10973-024-13543-4.
21. **Hassan M., Mahmoud M., El-Fattah A., Kandil S.** // *Ceram. Int.* 2016. V. 42. P. 3725–3744. DOI: 10.1016/j.ceramint.2015.11.044.
22. **Nabiyouni M., Zhou H., Luchini T., Bhaduri S.** // *Mater. Sci. Eng. C.* 2014. V. 37. P. 363-368. DOI: 10.1016/j.msec.2014.01.018.

23. **Asra D., Sari Y., Dahlan K.** // *IOP Conf. Ser. Earth Environ. Sci.* 2018. V. 187. P. 012016. DOI: 10.1088/1755-1315/187/1/012016.
24. **Teptereva G.A., Chetvertneva I.A., Movsumzade E.M., Sevastyanova M.V., Baulin O.A., Loginova M.E., Pakhomov S.I., Karimov E.H., Egorov M.P., Nifantyev N.E., Evstigneev E.I., Vasiliev A.V., Voloshin A.I., Nosov V.V., Dokichev V.A., Fakhreeva A.V., Babaev E.R., Rogovina S.Z., Berlin A.A., Kolchina G.Y., Voronov M.S., Staroverov D.V., Kozlovsky I.A., Kozlovsky R.A., Tarasova N.P., Zanin A.A., Krivoborodov E.G., Karimov O.K., Flid V.R.** // *ChemChemTech[Izv. Vyssh. Uchebn. Zaved. Khim. Khim. Tekhnol.]*. 2021. V. 64. N 9. P. 4-121 (in Russian). DOI: 10.6060/ivkkt.20216409.6465. **Тептерева Г.А., Пахомов С.И., Четвертнева И.А., Каримов Э.Х., Егоров М.П., Мовсумзаде Э.М., Евстигнеев Э.И., Васильев А.В., Севастьянова М.В., Волошин А.И., Нифантьев Н.Э., Носов В.В., Докичев В.А., Бабаев Э.Р., Роговина С.З., Берлин А.А., Фахреева А.В., Баулин О.А., Колчина Г.Ю., Воронов М.С., Староверов Д.В., Козловский И.А., Козловский Р.А., Тарасова Н.П., Занин А.А., Кривобородов Е.Г., Каримов О.Х., Флид В.Р., ЛогиноваМ.Е.** // *Изв. вузов. Химия и хим. технология.* 2021. Т. 64. Вып. 9. С. 4-121**.**
25. **Chaikina M., Bulina N., Prosanov I., Ishchenko A.** // *Cryst*. 2023. V. 13. P. 1264. DOI: 10.3390/cryst13081264.
26. **Akram M., Alshemary A., Goh Y. F., Ibrahim A., Lintang H., Hussain R.** // *Mat. Sci. Eng. C.* 2015. V. 56. P. 356–362. DOI: 10.1016/j.msec.2015.06.040.
27. **Vandeginste V., Cowan C., Gomes R., Hassan T., Titman J.** // *J. Hazard. Mat.* 2020. V. 389. P. 122150. DOI: 10.1016/j.jhazmat.2020.122150.
28. **Ebrahimi-Kahrizsangi R., Nasiri-Tabrizi B., Chami A.** // *Solid State Sci.* 2010. V. 12. P. 1645–1651. DOI: 10.1016/j.solidstatesciences.2010.07.017.
29. **Zhou H., Yang L., Gbureck U., Bhaduri S., Sikder P.** // *Acta Biomater*. 2021. V. 127. P. 41–55. DOI: 10.1016/j.actbio.2021.03.050.
30. **Xin-bo X., Miao-miao C., Feng X., Zou J., Xie-rong Z.** // *Surf. Coat. Techn*. 2015. V. 275. P. 69–74. DOI: 10.1016/j.surfcoat.2015.05.038.
31. **Shalini T., Rakkesh R., Bargavi P., Balakumar S.** // *Surf. Interfaces.* 2023. V. 40. P. 103089. DOI: 10.1016/j.surfin.2023.103089.

Поступила в редакцию 03.03.2025
Принята к опубликованию 14.05.2025

Received 03.03.2025
Accepted 14.05.2025